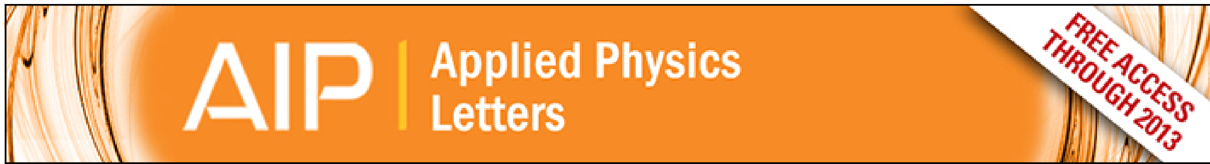

The effects of three-dimensional shaping of vertically aligned carbon-nanotube contacts for micro-electro-mechanical switches

Masoud Dahmardeh, Mehran Vahdani Moghaddam, Min Hian Tee, Alireza Nojeh, and Kenichi Takahata

Citation: Applied Physics Letters **103**, 231606 (2013); doi: 10.1063/1.4844695
View online: http://dx.doi.org/10.1063/1.4844695
View Table of Contents: http://scitation.aip.org/content/aip/journal/apl/103/23?ver=pdfcov
Published by the AIP Publishing

Re-register for Table of Content Alerts

Create a profile.

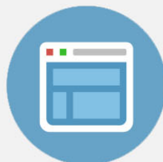

Sign up today!

This article is copyrighted as indicated in the article. Reuse of AIP content is subject to the terms at: http://scitation.aip.org/termsconditions. Downloaded to IP: 137.82.251.158 On: Tue, 24 Dec 2013 22:27:59

The effects of three-dimensional shaping of vertically aligned carbon-nanotube contacts for micro-electro-mechanical switches

Masoud Dahmardeh,[1] Mehran Vahdani Moghaddam,[1] Min Hian Tee,[2] Alireza Nojeh,[1,a)] and Kenichi Takahata[1,b)]
[1]*Department of Electrical and Computer Engineering, University of British Columbia, Vancouver, British Columbia V6T 1Z4, Canada*
[2]*Department of Mechanical Engineering, University of British Columbia, Vancouver, British Columbia V6T 1Z4, Canada*

(Received 30 October 2013; accepted 19 November 2013; published online 6 December 2013)

A micro-electro-mechanical switch integrated with vertically aligned carbon nanotubes (CNTs) as the contact material is presented. Arrays of the CNTs are three-dimensionally micropatterned using a pulsed micro-discharge process to have tapered contact surfaces with controlled angles, achieving maximized contact areas, while providing contact resistances in the 10 Ω range with an enhanced current capacity. A shape-memory-alloy actuator is integrated to demonstrate stable switching for $\sim 1.4 \times 10^6$ ON-OFF cycles with no sign of damage. The results prove that post-growth micropatterning of CNTs is a promising path to improved and reliable micro contact switches enabled by arrayed CNT contacts for high-power applications. © *2013 AIP Publishing LLC*. [http://dx.doi.org/10.1063/1.4844695]

Carbon nanotubes (CNTs) have attracted significant interest in the past two decades.[1–3] The ability to grow arrays of vertically aligned carbon nanotubes, so called CNT forests, through chemical vapor deposition (CVD) opened up opportunities to develop different types of advanced devices enabled by the material.[4,5] Owing to the unique and superior characteristics of the CNT forest in terms of mechanical,[6] electrical,[7] thermal,[8] chemical,[9] and optical[10,11] properties, the integration of the material into micro-electro-mechanical systems (MEMS) is a very attractive approach to advancing the functionality and performance of the devices. A key in facilitating MEMS applications of the material is the ability to pattern the material in a batch mode with high precision and high reproducibility. The CVD growth of patterned CNT forests has been implemented using pre-patterned catalyst layers defined by photolithography,[12,13] electron beam lithography,[14,15] soft mask,[16,17] and laser etching.[18] Patterning CNT forests during or after the growth using shadow mask,[7] mold,[19] laser etching through mask,[20] and densification[21,22] has been presented. The mentioned techniques are, however, primarily for the formation of two-dimensional types of patterns (with uniform heights). Laser micromachining has been reported to shape CNT forests for different applications[23–26] while exhibiting inherent limitations including tapered sidewalls, lack of high-precision depth control, and thermal damage.[27] Through previous studies, we developed free-form, three-dimensional (3D) patterning methods for CNT forests based on dry micro-electro-discharge machining (μEDM)[28] and reported the mechanism and characteristics of the process.[29–31] The 3D-pattened CNT forests are being utilized to realize high-performance devices such as field-emitters[7,32] and AFM scanning probes,[33] extending their application opportunities to other areas, including microfluidics,[34] gas sensors,[35,36] energy absorbing coatings,[6] and heat sinks.[25,37]

Another promising area to which the CNT forest could make a significant contribution is electrical contact switches. CNTs, with high current capacity of more than 10^9 A/cm^2,[38,39] low resistivity of 10^{-4} Ω cm^2,[40] and large surface area in the form of forests,[41] are good candidates for interconnect[42] and switching[43] applications. We previously developed a MEMS contact switch integrated with CNT forests that were used as the electrical contact material for high-power micro relay applications.[44] The switch, operated using a micromachined shape-memory-alloy (SMA) actuator, was demonstrated to show stable switching for over 1×10^6 cycles. However, it exhibited relatively high ON-state resistances ($\sim$500 Ω). The main cause of the high resistance is associated with the real contact area between the metallic electrode and the CNT forest contact as will be described later. The present work reports 3D micropatterning of the CNT-forests contact enabled by the dry μEDM process as a very effective route to addressing the issues related to the contact area, hence improving the conductance of the switch. Lowering the contact resistance leads to improvements in signal current (I_{sig}) capacity and power loss.

The micro contact switch developed is normally open and integrated with a micro-patterned CNT forest that serves as the electrical contact material. The switching operation is controlled with a SMA cantilever actuator that is thermally operated using a resistive heater integrated on the device. As shown in Fig. 1(a), the SMA cantilever structure is coated with a stress layer of SiO_2 that bends the structure upward in its martensite (cold) state at room temperature and is vertically actuated downward when heated to enter the austenite (hot) state of the SMA. The signal terminals (terminals 1 and 2) are disconnected in the OFF state in which the cantilever is in the bent condition. Once the heater is activated (by applying a current through it) to reach the austenite threshold temperature of the SMA, the cantilever is actuated toward its

a)Electronic mail: anojeh@ece.ubc.ca
b)Electronic mail: takahata@ece.ubc.ca

 © 2013 AIP Publishing LLC

This article is copyrighted as indicated in the article. Reuse of AIP content is subject to the terms at: http://scitation.aip.org/termsconditions. Downloaded to IP: 137.82.251.158 On: Tue, 24 Dec 2013 22:27:59

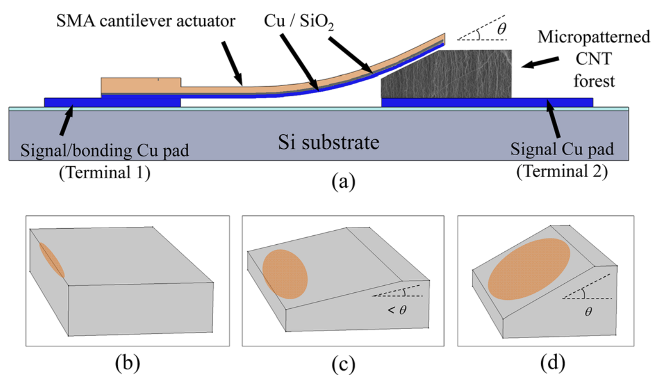

FIG. 1. (a) Cross sectional view of the switch device that integrates CNT-forest contact and SMA cantilever actuator that has its contact angle of θ; and three examples in the form of the CNT-forest contact; (b) as-grown CNT forest showing the possible real contact region with the angled cantilever only at a top corner as highlighted; (c) patterned forest having inclined contact surface with the contact angle less than θ leading to partial planar contact; (d) patterned forest having inclined contact surface with the contact angle equal to θ allowing full planar contact with the cantilever.

memorized flat shape, making a contact with the CNT forest and closing the switch, entering the ON state. This contact occurs at a top edge of the forest that generally has a rectangular cross section, rather than making a planar contact on the top surface of the forest, before the cantilever reaches its flat shape (i.e., the cantilever is still in a bent condition) as illustrated in Fig. 1(b). This contact condition (as in the case of the device previously reported[44]) significantly limits the real contact area, thus increasing the ON-state resistance of the switch. This study aims to investigate the effect of 3D shaping of the CNT-forest contacts toward improving the contact area and resistance. In particular, we utilize dry μEDM to achieve controlled, tapered surfaces with different angles in the CNT forests to evaluate the effect and maximize the contact area and hence the ON-state conductance of the switch. Fig. 1(c) displays the case where the angle of the sloped surface of the forest is smaller than the tip angle of the SMA cantilever at the touch-down condition, leading to a partial contact of the cantilever with the surface, whereas the case where the forest's slope angle matches the angle of the cantilever tip results in a full contact as illustrated in Fig. 1(d), thus, in principle, leading to a higher contact conductance.

The switch device is fabricated as follows. The heater and the pads are lithographically patterned in a 50-μm-thick Cu layer created on a lightly doped silicon wafer with a SiO_2 layer on top. A catalyst layer (Al_2O_3/Fe) is deposited on the corresponding Cu pad (terminal 2, Fig. 1(a)), on which multi-walled CNT forests are grown with heights of up to 200 μm using an ethylene-based atmospheric-pressure CVD process. The SMA film with 100-μm of thickness (adjusted using wet chemical etching) is patterned to form the cantilever structure with the bonding pad using a standard wet μEDM process.[45] The dimensions of the cantilever are defined to be the same as those of the device mentioned above.[44] A 4-μm-thick SiO_2 film, the stress layer for the SMA, is then deposited using plasma-enhanced CVD on the SMA cantilever, followed by evaporation of Cu (300 nm), the other electrode material that makes a direct contact with the CNTs when the switch is turned on. Further details of the fabrication described above can be found in our previous report.[44] The CNT forests grown on the heater substrates are then processed by dry μEDM to create inclined surfaces with different angles. These inclined surfaces are established by creating fine staircase profiles with varying depths and heights of the stair (this process will be described later). The SMA cantilever component is then aligned and bonded on the Cu pad (terminal 1, Fig. 1(a)) created on the substrate. This bonding is performed using a conductive dry-film adhesive (WaferGrip, Dynatex, Santa Rosa, CA, USA) that is inserted between the Cu pad on the substrate and the bonding pad created in the SMA cantilever. This assembly is annealed on a hotplate for 3–5 min at 120 °C while applying a force (of 10 N) to the bonding site of the SMA from its top surface; cooling the assembly down to room temperature completes the bonding process. In order to enhance the electrical connection of the bonded SMA cantilever to the Cu pad on the substrate, the bonding site is coated with a 200-nm-thick layer of Cu through a shadow mask.

Dry μEDM used for CNT-forest patterning was performed in air using a commercial 3-axis system with a positioning resolution of 100 nm (EM203, Samltec International, IL, USA). Details of the dry μEDM process are reported elsewhere.[28,29] The inclined surfaces of the forests with different angles were patterned using 300-μm-diameter cylindrical tungsten electrodes with flattened bottoms. The device substrate on which a CNT forest was formed was placed on the X-Y stage of the system to control its lateral position relative to the electrode tip, whereas the vertical position of the electrode was controlled with the Z stage of the system. The formation of these surfaces was achieved by creating staircase profiles, patterned by scanning the electrode over a CNT forest grown on the substrate along the X axis of the system, while making a common 5-μm step in the Z direction and a varying step in the Y direction in each scan, to define a certain angle of the staircase slope. Fabricated samples of the SMA cantilever in its cold state were measured to have an approximate angle of 26° between the free-end region of the cantilever and the substrate plane. This cantilever was integrated on the substrate so that its bottom surface of the free-end region was in close proximity to the CNT forest and made contact with a minimal displacement to minimize the switching time. Thus, the contact angle of the cantilever was presumed to be close to the initial angle (26°). Following this estimation, we patterned the sloped surfaces with an angle of 26°, as well as with other angles, 45° and 14°, to assess the dependence of the contact resistance on the angle of the forest's contact surface. These three angles were determined by setting the Y-axis step in the scanning μEDM process to be 10 μm, 20 μm, and 5 μm, respectively. Fig. 2(a) shows a patterned CNT forest with a 26°-angled surface that is observed to exhibit reasonably good flatness and uniformity, suggesting the effectiveness of the 3D dry μEDM process for the fabrication of CNT-forest contacts with customized 3D shapes. The overall images of the integrated device are shown in Fig. 2(b).

The electrical and thermomechanical characteristics of the fabricated devices as well as their dynamic behaviors were investigated using the set-up centered around an electronic workstation board (NI ELVIS II, National Instrument

This article is copyrighted as indicated in the article. Reuse of AIP content is subject to the terms at: http://scitation.aip.org/termsconditions. Downloaded to IP: 137.82.251.158 On: Tue, 24 Dec 2013 22:27:59

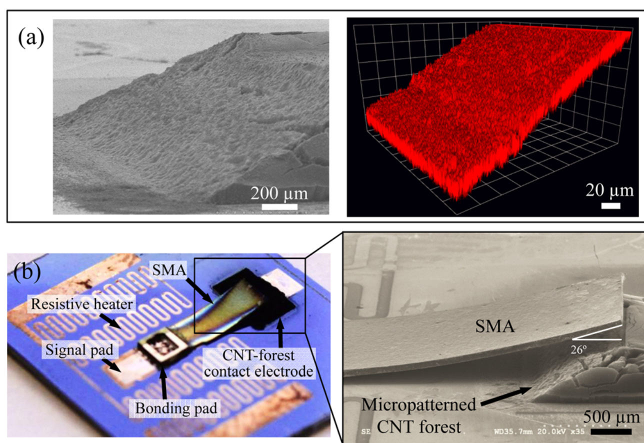

FIG. 2. (a) (left) Scanning electron microscope (SEM) image of patterned CNT-forest contact with 26°-angled surface and (right) the surface profile captured with laser scanning confocal microscope (Olympus FV1000, Japan); (b) (left) overall optical image of the developed switch device and (right) close-up SEM image of the integrated SMA cantilever and sloped CNT-forest contact.

Co., TX, USA) coupled with LabVIEW programs that were used for data acquisition. The NI board was also used to generate drive signals for the integrated heater to control the switch. The generated drive current was amplified to supply sufficient levels of current for the heater-switch operation. A thermocouple was used to record temperature of the heater circuit. A laser displacement sensor (LK-G32, Keyence, ON, Canada) with a sensing resolution of 10 nm and a spot size of 30 μm was used to capture the displacement of the SMA cantilever at its free end. The dependence of the ON-state contact resistance on the forest angle was first characterized using the devices fabricated to have 14°-, 26°-, and 45°-angled forest surfaces as described earlier; Fig. 3 shows a measurement result of the resistance recorded while applying a periodic signal voltage (V_{sig}) of 2.2 V (between terminals 1 and 2) for 10 s followed by an off time of 5 s. All the three devices were observed to exhibit OFF-state contact resistances on the order of 10 MΩ and ON-state contact resistances lower than those of the device with as-grown forest contacts (∼500 Ω).[44] Among them, as can be seen in Fig. 3, the device with the 26° contact angle showed the lowest contact resistance of ∼40 Ω (leading to I_{sig} of 55 mA), approximately 3-6× lower than the other two (14° and 45°) cases. This result verifies that the inclined CNT-forest contact with the angle tailored to that of the cantilever at its free end provides the minimal resistance, presumably due to an enhanced real contact area achieved by the particular configuration, whereas the devices with smaller or larger angles lead to smaller contact areas and hence higher resistances. Based on these observations, the rest of the experiments were carried out using the devices with the optimal, 26°-angled CNT-forest contacts.

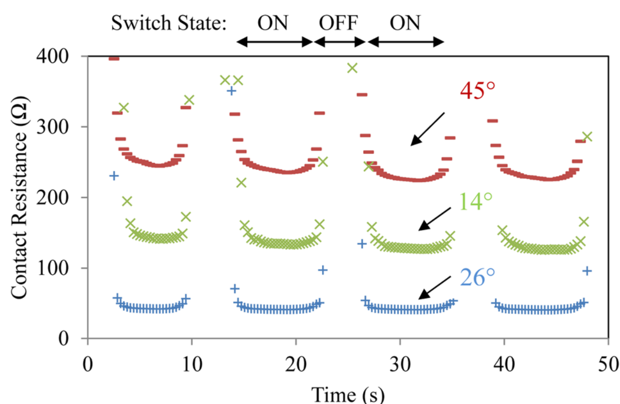

FIG. 3. Contact resistances of the switches using patterned CNT forests with three different slope angles measured at $V_{sig} = 2.2$ V.

The ON-state contact resistance of the defined device was observed to depend on the post-touchdown displacement of the SMA cantilever. As can be seen in the measurement result shown in Fig. 4(a), the resistance dropped abruptly at about 75-μm travel distance of the cantilever from the resting state, at which the cantilever made the first contact with the CNTs, and the resistance continued to drop as the cantilever was displaced further, most likely because the bottom electrode of the cantilever established more contact points with the tips of CNT arrays in the forest as displaced more. (The higher contact resistance (∼200 Ω) compared with the result shown in Fig. 3 is due to the dependence of the resistance on I_{sig}, as will be shown in Fig. 4(b), and a smaller I_{sig} (10 mA) used in this measurement.) Fig. 4(a) also indicates a reverse behavior of the displacement near its maximum point, which is potentially associated with a pivoting effect that lifted the tip of the cantilever caused by making a hard contact with the forest. These observations (displacement dependence of the resistance and the reverse behavior of the cantilever tip) are consistent with the results previously reported.[44]

Figs. 4(b)–4(d) show comparisons of electrical characteristics between the switch with the tapered CNT-forest contact and the one with bare CNT-forest contact.[44] The plots of measured contact resistances as a function of I_{sig} (up to ∼500 mA, Fig. 4(b)) clearly indicate that the former device exhibited substantially lower contact resistances than the latter for the entire I_{sig} range and achieved resistance values as low as 13.2 Ω at 515 mA. (The non-linear behavior of the resistance shown in Fig. 4(b) is also consistent with a previous result.[44]) Fig. 4(c) shows more rapid rise of I_{sig} with V_{sig} in the developed device due to its lower contact resistance, requiring less than half the voltage to sustain certain

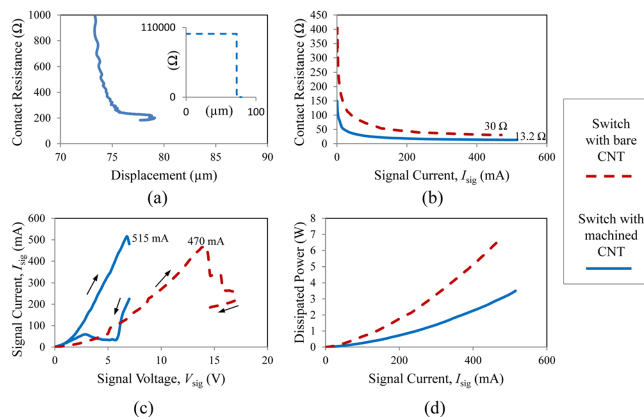

FIG. 4. (a) Dependence of contact resistance on the displacement (measured with I_{sig} of 10 mA). Comparisons between the switch with optimally angled CNT-forest contact and the one with bare forest contact for (b) contact resistance vs. I_{sig}, (c) I_{sig}-V_{sig}, and (d) dissipated power vs. I_{sig}.

This article is copyrighted as indicated in the article. Reuse of AIP content is subject to the terms at: http://scitation.aip.org/termsconditions. Downloaded to IP: 137.82.251.158 On: Tue, 24 Dec 2013 22:27:59

levels of I_{sig} (up to ~500 mA). The dissipated powers calculated from the results in Fig. 4(c) are plotted in Fig. 4(d); the angled contact switch conducts I_{sig} of, e.g., 450 mA at ~55% less dissipated power compared to the switch with a bare forest contact.

The temporal response of the developed device was characterized through automated sequential control of the SMA cantilever actuator. As the drive current was fed to the heater circuit, the cantilever actuator traveled down toward the tapered surface of the CNT forest and closed the switch by making contact with the surface. The LabVIEW program was arranged to maintain the drive current until the detected resistance reached a value as low as 200 Ω, after which the current was turned off to cool the cantilever, which was forced to go back to the original position caused by the stress layer and open the switch for the resistance to reach 1 MΩ. This ON-OFF cycle was repeated while recording the switch's resistance and the displacement of the cantilever tip (Fig. 5(a)). The initial displacement was ~80 μm, which decreased to 35–40 μm for the following cycles due to the threshold levels of the resistance set in the control sequence. One cycle was observed to complete in ~3 s with the setup used. A similar program (with a modified threshold level of the ON-state contact resistance of 60 Ω) was used to perform long-term operation of the developed device. Fig. 5(b) shows the ON-state contact resistance tracked during 1.4×10^6 cycles of switching operated with I_{sig} of 60 mA. As can be seen, the average resistance was measured to be almost within the range of 40–60 Ω for the entire test. As a comparison, the device with a bare forest contact[44] exhibited a resistance range of 600–700 Ω in long-term operation (~1×10^6 switching cycles with several-fold smaller I_{sig}). The improved contact area of the developed device, enabled by micropatterning of CNT-forest contacts, was demonstrated to achieve an order of magnitude lower contact resistance with a higher current carrying capacity, stably operating for a larger number of cycles with no sign of negative impact on the contact materials or the overall device.

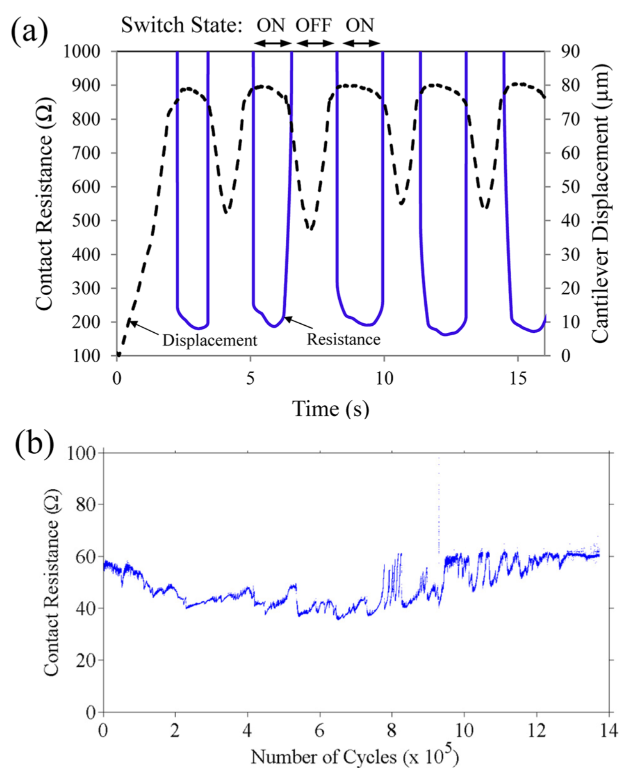

FIG. 5. (a) Temporal response of the fabricated switch device showing its contact resistance and cantilever's free-end displacement; (b) long-term trend of contact resistance for ~1.4×10^6 switching cycles demonstrating stable switching operation with an overall resistance range of 40–60 Ω.

In summary, we have studied the effect of 3D patterning of CNT forests toward advancing high-power micro-electromechanical switches enabled by integrated CNT-forest contacts. The experiments performed using fabricated devices verified that the approach improved the ON-state conductance and current carrying capacity of the switch, presumably because the μEDM-patterned forest surfaces with controlled angles maximized the real contact area, i.e., the number of contact points between the individual CNTs in the forest and the cantilever. The results observed with differently angled forest contacts supported this hypothesis. The electromechancial behaviors of the fabricated switch device with an optimal contact angle were characterized to reveal ON-state contact resistances as low as 13.2 Ω with I_{sig} of over 500 mA and suppressed power dissipations in the device. The stable operation of the device was demonstrated for switching cycles of ~1.4×10^6, with 10–17 × lower ON-state contact resistances than the device with a CNT-forest contact with a flat top surface.

This work was partially supported by the Natural Sciences and Engineering Research Council of Canada, the Canada Foundation for Innovation, the British Columbia Knowledge Development Fund, and the BCFRST Foundation/British Columbia Innovation Council. The authors thank Simon Wu for his assistance in figure preparation. K. Takahata was supported by the Canada Research Chairs program.

[1]S. Iijima, Nature **354**, 56 (1991).
[2]R. H. Baughman, A. A. Zakhidov, and W. A. de Heer, Science **297**, 787 (2002).
[3]M. F. L. De Volder, S. H. Tawfick, R. H. Baughman, and A. J. Hart, Science **339**, 535 (2013).
[4]Y. Hayamizu, T. Yamada, K. Mizuno, R. C. Davis, D. N. Futaba, M. Yumura, and K. Hata, Nat. Nanotechnol. **3**, 289 (2008).
[5]D. N. Hutchison, N. B. Morrill, Q. Aten, B. W. Turner, B. D. Jensen, L. L. Howell, R. R. Vanfleet, and R. C. Davis, J. Microelectromech. Syst. **19**, 75 (2010).
[6]A. Cao, P. L. Dickrell, W. G. Sawyer, M. N. Ghasemi-Nejhad, and P. M. Ajayan, Science **310**, 1307 (2005).
[7]S. Fan, Science **283**, 512 (1999).
[8]H. Huang, C. H. Liu, Y. Wu, and S. Fan, Adv. Mater. **17**, 1652 (2005).
[9]K. K. S. Lau, J. Bico, K. B. K. Teo, M. Chhowalla, G. A. J. Amaratunga, W. I. Milne, G. H. McKinley, and K. K. Gleason, Nano Lett. **3**, 1701 (2003).
[10]Y. Murakami, E. Einarsson, T. Edamura, and S. Maruyama, Phys. Rev. Lett. **94**, 087402 (2005).
[11]K.-C. Hsieh, T.-Y. Tsai, D. Wan, H.-L. Chen, and N.-H. Tai, ACS Nano **4**, 1327 (2010).
[12]J. I. Sohn, S. Lee, Y.-H. Song, S.-Y. Choi, K.-I. Cho, and K.-S. Nam, Appl. Phys. Lett. **78**, 901 (2001).
[13]O. Yaglioglu, R. Martens, A. J. Hart, and A. H. Slocum, Adv. Mater. **20**, 357 (2008).
[14]Z. F. Ren, Z. P. Huang, D. Z. Wang, J. G. Wen, J. W. Xu, J. H. Wang, L. E. Calvet, J. Chen, J. F. Klemic, and M. A. Reed, Appl. Phys. Lett. **75**, 1086 (1999).

This article is copyrighted as indicated in the article. Reuse of AIP content is subject to the terms at: http://scitation.aip.org/termsconditions. Downloaded to IP: 137.82.251.158 On: Tue, 24 Dec 2013 22:27:59

[15]K. B. K. Teo, M. Chhowalla, G. A. J. Amaratunga, W. I. Milne, D. G. Hasko, G. Pirio, P. Legagneux, F. Wyczisk, and D. Pribat, Appl. Phys. Lett. **79**, 1534 (2001).
[16]H. Kind, J.-M. Bonard, C. Emmenegger, L.-O. Nilsson, K. Hernadi, E. Maillard-Schaller, L. Schlapbach, L. Forró, and K. Kern, Adv. Mater. **11**, 1285 (1999).
[17]L. Nilsson, O. Groening, C. Emmenegger, O. Kuettel, E. Schaller, L. Schlapbach, H. Kind, J.-M. Bonard, and K. Kern, Appl. Phys. Lett. **76**, 2071 (2000).
[18]M. Terrones, N. Grobert, J. Olivares, J. P. Zhang, H. Terrones, K. Kordatos, W. K. Hsu, J. P. Hare, P. D. Townsend, K. Prassides, A. K. Cheetham, H. W. Kroto, and D. R. M. Walton, Nature **388**, 52–55 (1997).
[19]J. Li, C. Papadopoulos, J. M. Xu, and M. Moskovits, Appl. Phys. Lett. **75**, 367 (1999).
[20]F. C. Cheong, K. Y. Lim, C. H. Sow, J. Lin, and C. K. Ong, Nanotechnology **14**, 433 (2003).
[21]D. Jiang, T. Wang, S. Chen, L. Ye, and J. Liu, Microelectron. Eng. **103**, 177 (2013).
[22]T. Wang, D. Jiang, S. Chen, K. Jeppson, L. Ye, and J. Liu, Mater. Lett. **78**, 184 (2012).
[23]K. Y. Lim, C. H. Sow, J. Lin, F. C. Cheong, Z. X. Shen, J. T. L. Thong, K. C. Chin, and A. T. S. Wee, Adv. Mater. **15**, 300 (2003).
[24]Z. H. Lim and C.-H. Sow, Adv. Funct. Mater. **20**, 847 (2010).
[25]K. Kordás, G. Tóth, P. Moilanen, M. Kumpumaüki, J. Vaühaükangas, A. Uusimaüki, R. Vajtai, and P. M. Ajayan, Appl. Phys. Lett. **90**, 123105 (2007).
[26]W. H. Hung, R. Kumar, A. Bushmaker, S. B. Cronin, and M. J. Bronikowski, Appl. Phys. Lett. **91**, 093121 (2007).
[27]K. Jain and J. Chae, SPIE Newsroom, February 2, 2009.
[28]W. Khalid, M. S. M. Ali, M. Dahmardeh, Y. Choi, P. Yaghoobi, A. Nojeh, and K. Takahata, Diamond Relat. Mater. **19**, 1405 (2010).
[29]M. Dahmardeh, A. Nojeh, and K. Takahata, J. Appl. Phys. **109**, 093308 (2011).
[30]T. Saleh, M. Dahmardeh, A. Bsoul, A. Nojeh, and K. Takahata, J. Appl. Phys. **110**, 103305 (2011).
[31]T. Saleh, M. Dahmardeh, A. Nojeh, and K. Takahata, Carbon N. Y. **52**, 288 (2013).
[32]M. Vahdani Moghaddam, M. S. Sarwar, Z. Xiao, M. Dahmardeh, K. Takahata, and A. Nojeh, in *26th International Vacuum. Nanoelectronics Conference* (Roanoke, VA, USA, 2013), pp. 1–2.
[33]Z. Xiao, M. S. Sarwar, M. Dahmardeh, M. Vahdani Moghaddam, A. Nojeh, and K. Takahata, Appl. Phys. Lett. **103**, 171603 (2013).
[34]P. Joseph, C. Cottin-Bizonne, J.-M. Benoît, C. Ybert, C. Journet, P. Tabeling, and L. Bocquet, Phys. Rev. Lett. **97**, 156104 (2006).
[35]J. Kong, N. Franklin, C. Zhou, M. Chapline, S. Peng, K. Cho, and H. Dai, Science **287**, 622 (2000).
[36]S. Ammu, V. Dua, S. R. Agnihotra, S. P. Surwade, A. Phulgirkar, S. Patel, and S. K. Manohar, J. Am. Chem. Soc. **134**, 4553 (2012).
[37]Y. Fu, N. Nabiollahi, T. Wang, S. Wang, Z. Hu, B. Carlberg, Y. Zhang, X. Wang, and J. Liu, Nanotechnology **23**, 045304 (2012).
[38]B. Q. Wei, R. Vajtai, and P. M. Ajayan, Appl. Phys. Lett. **79**, 1172 (2001).
[39]Z. Yao, C. Kane, and C. Dekker, Phys. Rev. Lett. **84**, 2941 (2000).
[40]Y.-H. Li, J. Wei, X. Zhang, C. Xu, D. Wu, L. Lu, and B. Wei, Chem. Phys. Lett. **365**, 95 (2002).
[41]M. Park, B. A. Cola, T. Siegmund, J. Xu, M. R. Maschmann, T. S. Fisher, and H. Kim, Nanotechnology **17**, 2294 (2006).
[42]J. Robertson, G. Zhong, C. S. Esconjauregui, B. C. Bayer, C. Zhang, M. Fouquet, and S. Hofmann, Jpn. J. Appl. Phys., Part 1 **51**, 01AH01 (2012).
[43]J. Choi, J.-I. Lee, Y. Eun, M.-O. Kim, and J. Kim, Adv. Mater. **23**, 2231 (2011).
[44]M. Dahmardeh, M. S. Mohamed Ali, T. Saleh, T. M. Hian, M. V. Moghaddam, A. Nojeh, and K. Takahata, Phys. Status Solidi **210**, 631 (2013).
[45]K. Takahata, in *Micro Electronic and Mechnical Systems* (InTech, 2009), p. 386.

This article is copyrighted as indicated in the article. Reuse of AIP content is subject to the terms at: http://scitation.aip.org/termsconditions. Downloaded to IP: 137.82.251.158 On: Tue, 24 Dec 2013 22:27:59